Role of Membrane Tension Sensitive Endocytosis and Rho GTPases in the Uptake of the Alzheimer's Disease Peptide Aß(1-42)

ACS Chemical Neuroscience

pubs.acs.org/chemneuro

Research Article

Role of Membrane Tension Sensitive Endocytosis and Rho GTPases in the Uptake of the Alzheimer's Disease Peptide Aβ(1-42)

Emelie Wesén, Richard Lundmark, and Elin K. Esbjörner*

Cite This: *ACS Chem. Neurosci.* 2020, 11, 1925−1936

Read Online

ACCESS | Metrics & More | Article Recommendations | Supporting Information

ABSTRACT: Intraneuronal accumulation of amyloid-β (Aβ) is an early pathological signum of Alzheimer's disease, and compartments of the endolysosomal system have been implicated in both seeding and cell−cell propagation of Aβ aggregation. We have studied how clathrin-independent mechanisms contribute to Aβ endocytosis, exploring pathways that are sensitive to changes in membrane tension and the regulation of Rho GTPases. Using live cell confocal microscopy and flow cytometry, we show the uptake of monomeric Aβ(1-42) into endocytic vesicles and vacuole-like dilations, following relaxation of osmotic pressure-induced cell membrane tension. This indicates Aβ(1-42) uptake via clathrin independent carriers (CLICs), although overexpression of the bar-domain protein GRAF1, a key regulator of CLICs, had no apparent effect. We furthermore report reduced Aβ(1-42) uptake following overexpression of constitutively active forms of the Rho GTPases Cdc42 and RhoA, whereas modulation of Rac1, which is linked to macropinosome formation, had no effect. Our results confirm that uptake of Aβ(1-42) is clathrin- and dynamin-independent and point to the involvement of a new and distinct clathrin-independent endocytic mechanism which is similar to uptake via CLICs or macropinocytosis but that also appear to involve yet uncharacterized molecular players.

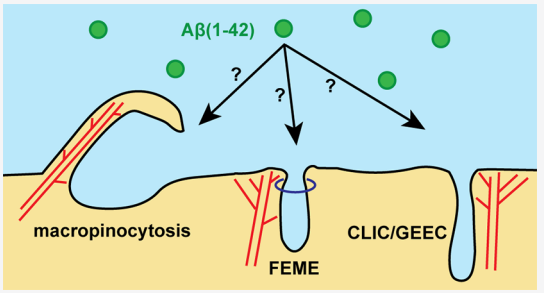

KEYWORDS: *Amyloid-β, Aβ(1-42), Alzheimer's disease, cellular uptake, clathrin-independent endocytosis (CIE), uptake mechanism*

INTRODUCTION

Alzheimer's disease (AD) is characterized by the aggregation of amyloid-β (Aβ) peptides resulting in the formation of extracellular plaque deposits in the brain[1,2] alongside the formation of intracellular neurofibrillary tau tangles.[3] Aβ has been suggested as a causative agent of AD pathology;[4] many familial forms of AD are associated with mutations that enhance the aggregation propensity of Aβ or alter, disfavorably, its production, processing, and clearance.[5−9] Aβ is formed by proteolytic cleavage of the amyloid precursor protein (APP).[10] This predominantly occurs in endolysosomal organelles whereupon Aβ can be secreted or retained.[11] Extracellular Aβ can efficiently enter cultured cells via endocytosis.[12−15] It reportedly also enters neurons following tail vein injections into mice with a compromised blood brain barrier,[16] suggesting that the intra- and extracellular Aβ pools are dynamically related.[17] The confinement of Aβ in endolysosomal vesicles subjects the peptide to aggregation promoting conditions, including low pH[18] and the presence of lipid membranes.[19] Accordingly, we and others have shown that endocytosed Aβ is aggregating inside living cells,[14,20] and it has been suggested that endolysosomal compartments could serve as initial sites of Aβ seed formation.[15,21] Interestingly, in this regard, intraneuronal buildup of Aβ appear as one of the earliest signs of AD, typically manifesting before the formation of extracellular plaques.[22−24] For these reasons, as well as the putative importance of endocytosis and the endolysosomal system in the prion-like cell-cell propagation of Aβ aggregation,[25,26] it is important to better understand how Aβ peptides are endocytosed and accumulated.

We have previously shown that both Aβ(1-40) and Aβ(1-42) (the two most commonly occurring Aβ isoforms[11]) are taken up via clathrin- and dynamin-independent endocytosis when applied to cultured cells in monomeric form;[13] this uptake was furthermore perturbed by actin depolymerization and pharmacological inhibitors of macropinocytosis. We and others have also demonstrated an important role for cell surface proteoglycans.[20,27−29] In this study, we further explore Aβ uptake, focusing on clathrin-independent endocytosis (CIE) mechanisms. We also explore the regulatory role of small signaling G-proteins of the Rho GTPase family, due to their key role in regulating actin dynamics during CIE[30] and their putative function as target molecules in AD pathogenesis.[31]

Received: January 30, 2020
Accepted: June 4, 2020
Published: June 4, 2020

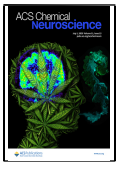

While the mechanisms and functions of clathrin-mediated endocytosis (CME) have been well studied in many physiological contexts,[32] CIE mechanisms remain much less well-defined due to their diversity and complexity.[33] It is not yet understood how many distinct CIE mechanisms a cell actually has nor is it clear how extensively these paths are used in different cell types. Reports range from almost exclusive use of CME,[34] to situations where the majority of the cellular endocytic volume is internalized via CIE.[35] CIE is, importantly, active in neurons, contributing to cargo uptake and fast regulation of membrane turnover at synapses[36] where Aβ peptides are also present. In addition to the implicated role in Aβ monomer uptake,[13,20] CIE also contributes to the neuronal internalization of the APP-processing enzyme BACE1,[37] the amyloidogenic human PrP protein,[38] as well as several types of amyloid oligomers and fibrils.[39,40]

The molecular and mechanistic classification of CIE has been complicated by the apparent lack of specific cargoes and exclusive regulators.[33] Nonetheless, at least three distinct pathways exist, all regulated by activating/deactivating cycling of specific small signaling G-proteins of the Rho GTPase family[30,41] (Figure 1). Macropinocytosis is initiated by large

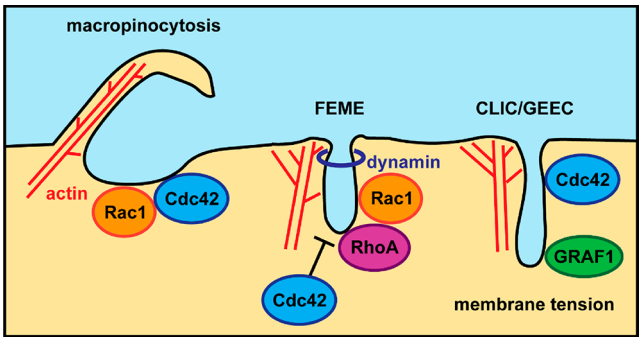

Figure 1. Clathrin-independent endocytosis (CIE). Uptake via the CIE paths macropinocytosis, FEME, and CLIC/GEEC, highlighting the respective involvement of the Rho GTPases Cdc42, Rac1 and RhoA, as well as that of GRAF1 and sensitivity to changes in membrane tension.

(micrometer size-range), actin-driven membrane protrusions and is activated by specific signals,[42] such as growth factors, chemokines,[43] cationic peptides,[44] and amyloid assemblies.[39] Rac1 activation is highly coupled to macropinocytosis.[30] Fast endophilin-mediated endocytosis (FEME)[45] results from cargo capture and local membrane bending assisted by the endophilin BAR-domain and other cytosolic proteins.[41] FEME is important in assisting fast membrane recycling at the synapse[46] and occurs under the regulatory control of dynamin as well as the Rho GTPases Rac1 and RhoA. It is furthermore activated upon inhibition of Cdc42.[45] The dynamin independence of Aβ endocytosis[13] suggests, however, that FEME is not involved; notably this was further reinforced by our study. Finally, CIE uptake can also occur via clathrin-independent carriers (CLICs) into glycosylphosphatidylinositol (GPI)-anchored protein enriched endocytic compartments (GEECs; CLIC/GEEC).[47,48] CLIC/GEEC is a constitutive and cargo clustering driven pathway important for the uptake of GPI-anchored proteins, glycosylated cargoes, certain toxins, and glycosphingolipids.[41] CLICs are furthermore involved in the endocytosis of the brain abundant lipid GM1, which is a well-recognized Aβ binding partner.[49] CLIC formation is regulated by Cdc42, and the formation of at least one subpopulation of CLICs is also dependent on the GTPase-regulatory and BAR-domain containing protein GRAF1.[47,50,51]

Endocytosis via CLIC/GEEC, but also via macropinocytosis, is modulated by changes in plasma membrane tension,[52−54] and the mechanisms are upregulated under conditions where cells need to rapidly internalize excess plasma membrane. Their involvement in cargo uptake can therefore be explored by altering the tonicity of the cell culture medium[51,53,54] as explored here.

The small Rho GTPases in this study are not only important regulators of CIE, they are also involved in both neuronal development and neurodegeneration, and their activity (specifically that of Rac1 and RhoA) has been observed to decrease in the brains of patients with AD.[55] Furthermore, Rac1 activation increases the production of Aβ from APP and results in hyperphosphorylation of tau, thereby providing a possible link between these two AD-relevant pathological hallmarks.[56] It has also been suggested that soluble Aβ(1-40) peptides can reduce neurite length in a neuroblastoma model by inducing RhoA activity,[57] whereas application of fibrillar Aβ(1-42) to neurons has been reported to result in dysregulated actin polymerization through altered activity of Rac1 and Cdc42.[58] Furthermore, Aβ(1-42) oligomers have been observed to exert cellular toxicity in a RhoA-dependent manner, following internalization.[59] By being key regulators of several AD-related signals, Rho GTPases have also been suggested as possible therapeutic targets.[60] Thus, effects of Aβ internalization on Rho GTPase regulation have been established in several AD-relevant contexts, but it has not yet been explored how modulation of various Rho GTPases *per se* affect the clathrin-independent endocytic uptake of Aβ itself. Lastly, several reports link AD to dysregulated cholesterol metabolism,[61] and it has been shown in a variety of *in vitro* biophysical contexts that amyloid assemblies, including Aβ, are in themselves potent modulators of membrane organization, integrity, and bending,[62] suggesting they might have direct, cargo-mediated effects on various types of CIE.

This study extends our previous work on Aβ endocytosis by focusing specifically on the role of CIE in the uptake of Aβ(1-42) monomers. We probe CIE mechanisms by modulating cell membrane tension,[52] Rho GTPase expression (Cdc42, Rac1 and RhoA), and the activity of the CLIC/GEEC specific GTPase activating protein GRAF1.[50] We show that the uptake of Aβ(1-42), supplied to human neuroblastoma SH-SY5Y cells, is catalyzed upon relief of hypotonic media-induced plasma membrane tension via a mechanism that is under regulatory control of the small GTPases Cdc42 and RhoA but not Rac1. These findings suggest that actin polymerization is highly important but that internalization is not via macropinocytosis in its most classical description. Furthermore, Aβ(1-42), despite being previously shown to occur at the leading edge of cells and in areas of high membrane ruffling, was found to be independent of GRAF1, suggesting that its CIE uptake involve other, yet unidentified, endocytic membrane sculpting proteins. Altogether, this work has revealed new insights into how components of CIE are related to the endocytosis of Aβ(1-42) and, significantly, pointed out that AD-relevant dysregulations of Rho GTPase activities could importantly influence the extent of intraneuronal Aβ accumulation.

https://dx.doi.org/10.1021/acschemneuro.0c00053
ACS Chem. Neurosci. 2020, 11, 1925−1936

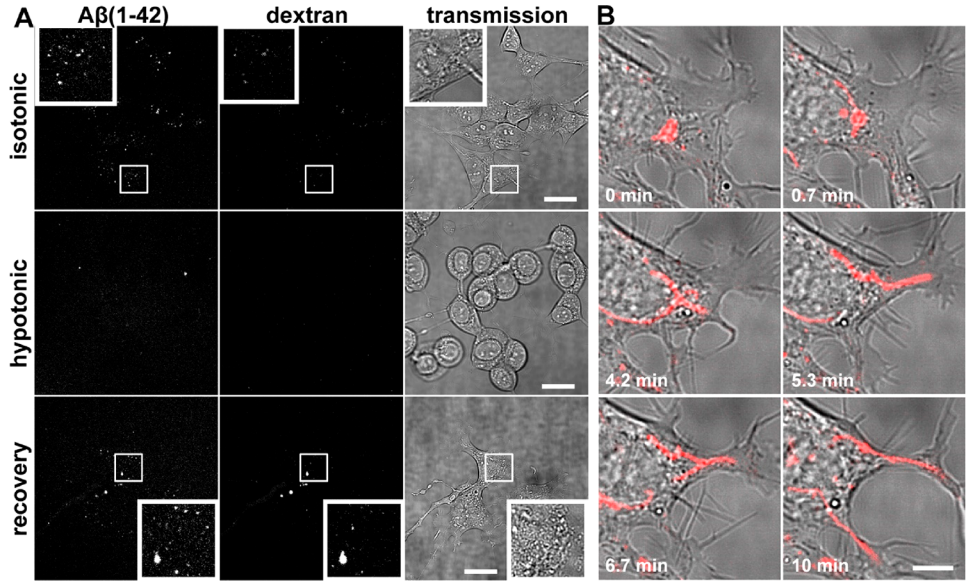

Figure 2. Cellular uptake of Aβ(1-42) in cells exposed to a hypotonic shock. (A) Confocal microscopy images of SH-SY5Y cells incubated with 2 μM HF488-labeled Aβ(1-42) and 250 μg/mL AF647-labeled dextran 10 kDa for 10 min during either isotonic or hypotonic (75% MQ water, 25% cell culture medium) conditions. Recovery denotes cells transferred back to isotonic media after the 10 min hypotonic treatment, at which point Aβ(1-42) and dextran was also added. The scale bars in part A represent 20 μm. The isotonic/hypotonic/recovery images have been acquired with identical settings and post-treated in the same manner, i.e., the displayed intensities are comparable for Aβ(1-42) and dextran, respectively. Inserts display zoomed areas. (B) Zoomed images of one representative cell with AF647-labeled dextran 10 kDa-filled VLDs (internalized during exposure to 250 μg/mL dextran for 10 min at recovery conditions). The time-lapse was started after the 10 min recovery period and a 1× wash, and the cells were imaged by confocal microscopy. The scale bar is 5 μm. The time lapse movie is displayed as Supplementary Movie 4.

RESULTS AND DISCUSSION

Cellular Uptake of Monomeric Aβ(1-42) Is Increased by the Alleviation of Hypotonic-Media Induced Membrane Tension. Uptake into endolysosomal compartments and subsequent intraneuronal accumulation have been implicated in both seeding and cell−cell propagation of Aβ(1-42). Previous work has shown that uptake of monomeric Aβ(1-42) is clathrin-independent,[13] and in order to further map out the involved endocytic paths and regulators, we here focus on clathrin-independent endocytosis (CIE).

First, we explored how modulation of the plasma membrane tension, achieved by altering the tonicity of the incubation medium,[63−65] influenced the cellular uptake of Aβ(1-42), applied in highly monomeric form, to cultured SH-SY5Y neuroblastoma cells. Such acute changes in membrane tension have previously been described in studies on CLIC/GEEC in HeLa cells[51,54] and is an approach to mimic the dynamic changes in membrane tension that occur at cell membrane protusions.[54,66] In previous studies, uptake via CLIC/GEEC was found to be upregulated following the sudden reduction in membrane tension that occur when cells are transferred from hypotonic medium to isotonic medium.[51,54] A recent study using mouse-derived myoblasts suggests that also macropinocytosis can be affected by these conditions;[53] hence, exposing cells to a sudden reduction in membrane tension is an approach to probe for uptake via the CLIC/GEEC pathway and/or macropinocytosis.

In our experiments, cells were sequentially subjected to isotonic (cell culture medium), hypotonic (25% cell culture medium, 75% MQ water) and recovery (transfer from hypotonic to cell culture medium) conditions for 10 min each while simultaneously being exposed to highly monomeric preparations[13] of fluorescently labeled (HiLyteFluor488 (HF488)) Aβ(1-42) peptides and the fluid phase marker dextran 10 kDa (labeled with AlexaFluor647 (AF647)). Cells were imaged by time lapse confocal microscopy (Supplementary Movies 1−3) after washing away external, non-internalized peptide and dextran at the end of each 10 min incubation period (Figure 2A). Under isotonic conditions, the formation of small endosomal vesicles containing Aβ(1-42) was observed (Supplementary Movie 1 and Figure 2A, top row), consistent with previous reports by us and others.[12−15] The fluorescence intensities in the movies and images are weak, due to the short incubation period and low Aβ(1-42) concentration (2 μM); also the uptake of dextran, which is a nonspecific fluid phase endocytosis marker,[67] is low. During exposure to hypotonic conditions, the cells expanded and rolled up due to an osmotic pressure-induced increase in cell volume. Previous studies have shown that this is accompanied by an increase in plasma membrane tension,[63−65] which was increased by a factor of 3 (from 0.04 to 0.12 mN/m) in molluscan neurons exposed to hypotonic medium (50% MQ).[64] In our experiments, we observe little or no internalization of Aβ(1-42) and dextran (Supplementary Movie 2 and Figure 2A, middle row). During re-exposure to isotonic conditions (recovery), the cells readopted normal morphology and resumed to internalize Aβ(1-42) (Figure 2A, bottom row) into both smaller endosomal vesicles and larger structures. The latter are consistent in appearance with the vacuole-like dilations (VLDs) that have been reported during similar membrane tension changing conditions in other studies,[52,68] including those using neurons.[69,70] Uptake of the CME-ligand[71] transferrin (Trf) was blocked under hypotonic treatment and remained low throughout the recovery period (Supplementary Figure S1), demonstrating that CME is not upregulated upon a reduction in membrane tension in SH-SY5Y cells, in agreement with a previous study using CHO cells.[52] Uptake of dextran was also induced by recovery from

https://dx.doi.org/10.1021/acschemneuro.0c00053
ACS Chem. Neurosci. 2020, 11, 1925−1936

the hypotonic treatment (Figure 2A, bottom row). Contrasting to Aβ(1-42), this fluid-phase marker only appeared to internalize into VLDs (Supplementary Movie 3), indicating a behavioral difference and a higher degree of specificity of Aβ(1-42) towards small vesicles. The small Aβ(1-42) containing endosomes could either originate from a specific upregulation of a distinctive endocytic pathway or from a specific type of uptake from the VLDs as such. We therefore monitored the faith of the dextran-containing VLDs in the SH-SY5Y cells by time lapse microscopy (Figure 2B, Supplementary Movie 4; recordings started when the cells had been kept for 10 min in the recovery phase), observing both tubulation and concurrent fission of the tubules. This confirms that the VLDs are internal and dynamic structures that are being degraded and eventually eliminated by the cell.[54] An interesting observation in this regard is that the VLDs we observe in SH-SY5Y cells persist longer (in general >10 min), compared to VLDs in HeLa or mouse embryonic fibroblasts cells (where they disappear within minutes);[54,68] the number of VLDs per SH-SY5Y cell also appears to be high. It is possible that these differences stem from the fact that SH-SY5Y cells, like all neuroblastoma cells, lack caveolin-1[72] and therefore cannot regulate their cell surface in response to membrane tension reduction by caveolae formation.[33,41] We also characterized the response of SH-SY5Y cells to the acute changes in membrane tension applied in our experiments by imaging the actin cytoskeleton in cells transfected with CellLight Actin-GFP (Supplementary Movie 5 and Figure S2). While actin filaments were clearly visible in cells before the hypotonic treatment, these structures rapidly disassembled following addition of MQ, in agreement with previous reports.[63,73] Furthermore, within the timespan of the recovery experiment, the actin filaments did not completely re-establish; instead more punctate filaments were formed.

To quantitate how changes in membrane tension affected cell uptake of Aβ(1-42), Trf, and dextran, we used flow cytometry. Figure 3A shows mean fluorescence intensities (normalized relative to uptake in isotonic media), supporting the imaging data (Figure 2A and Supplementary Figure S1). Interestingly, the extent of Aβ(1-42) uptake during the recovery phase merely doubles, whereas the uptake of dextran is increased ~8 times, suggesting a difference in uptake mechanism and membrane tension dependence of the two macromolecules. This was further substantiated by the observation that the uptake of Aβ(1-42) and dextran during recovery has different linear concentration dependence (Figure 3B, Supplementary Figure S3); the concentration dependence for Aβ(1-42) has a slope of 4.3 ± 0.7 compared to 13.5 ± 2.1 for dextran).

We next explored how the uptake of Aβ(1-42) and dextran during recovery depended on the magnitude of the hypotonic shock, probing also smaller changes in membrane tension (Figure 3C,D). Aβ(1-42) and dextran have very similar trends, and clear effects are only observed above 50% MQ, which has also been applied in other studies.[51,54] Exposure of the cells to hypertonic media (addition of 100 mM NaCl to the culture medium) to reduce membrane tension did not increase Aβ(1-42) or dextran uptake (Supplementary Figure S4), suggesting that uptake during membrane tension reduction is directly related to the cell's need to reduce its cell membrane surface area.

Cellular Uptake of Aβ(1-42) Is Independent of GRAF1. Building on the results above, demonstrating a membrane tension-sensitive endocytosis of Aβ(1-42), we next explored if the uptake was mediated via GRAF1-dependent CLIC/GEEC. We used an engineered HeLa Flp-In T-REx cell line with an inducible expression of GFP-GRAF1,[54] but it has also been shown that GRAF1 is constitutively expressed and thus relevant for CIE in SH-SY5Y cells.[50] The HeLa cell line was transfected with mCherry-tagged Cdc42 (WT and dominant active (DA) Q61L mutant). Upon doxycycline-induced low level expression of GFP-GRAF1, punctuate and tubular GRAF1-positive structures appeared in cells expressing DA Cdc42 Q61L but not Cdc42 WT, as reported by Vidal-Quadras et al.[54] CLIC/GEEC ligands are expected to be trapped in these GRAF1-structures but unable to transit further due to the DA Cdc42 Q61L overexpression, thus enabling visualization of GRAF1-mediated uptake via CLIC/GEEC, which is otherwise a very fast event.[35] Cells were incubated with 1 μM Aβ(1-42) for 40 min, resulting in the formation of Aβ(1-42)-containing endosomal vesicles that did not colocalize with, or appear to display any similar intracellular distribution pattern as, GRAF1 in cells transfected with Cdc42 Q61L (Figure 4A). Since it is possible that the lack of colocalization between Aβ(1-42) and GRAF1 is due to the fairly long incubation time (40 min; needed to achieve high signal-to-noise images of intracellular Aβ(1-42) in this case), it cannot be excluded that Aβ(1-42) has been trafficked from CLICs to downstream endosomal organelles by the time of analysis. Therefore, we also exposed cells to a shorter incubation pulse (15 min) at a higher peptide concentration

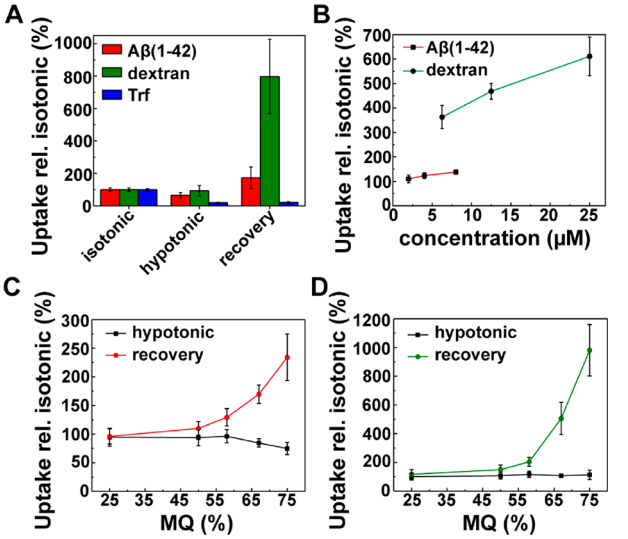

Figure 3. Cellular uptake of Aβ(1-42) is influenced by changes in membrane tension. (A) Quantification of cellular uptake of 2 μM HF488-labeled Aβ(1-42), 250 μg/mL AF647-labeled dextran 10 kDa or 5 μg/mL AF488-labeled transferrin (Trf) during 10 min isotonic, hypotonic (75% MQ) and recovery conditions, as explained in Figure 2A. N = 8 (Aβ(1-42) and dextran) or N = 4 (Trf), n = 3−4. (B) Cellular uptake as a function of concentration of HF488-labeled Aβ(1-42) and AF647-labeled dextran, monitored during the 10 min recovery period after an hypotonic shock (75% MQ), as explained in Figure 2A, n = 4. (C,D) Cellular uptake of (C) HF488-labeled Aβ(1-42) and (D) AF647-labeled dextran in cells exposed to a hypotonic shock following the same experimental procedure as in part A but with varying content of MQ in the hypotonic medium (N = 3−4, n = 3−4). (A−D) Cells were analyzed by flow cytometry, and uptake is reported as mean cellular uptake relative to uptake in cells exposed to isotonic conditions.

https://dx.doi.org/10.1021/acschemneuro.0c00053
ACS Chem. Neurosci. 2020, 11, 1925−1936

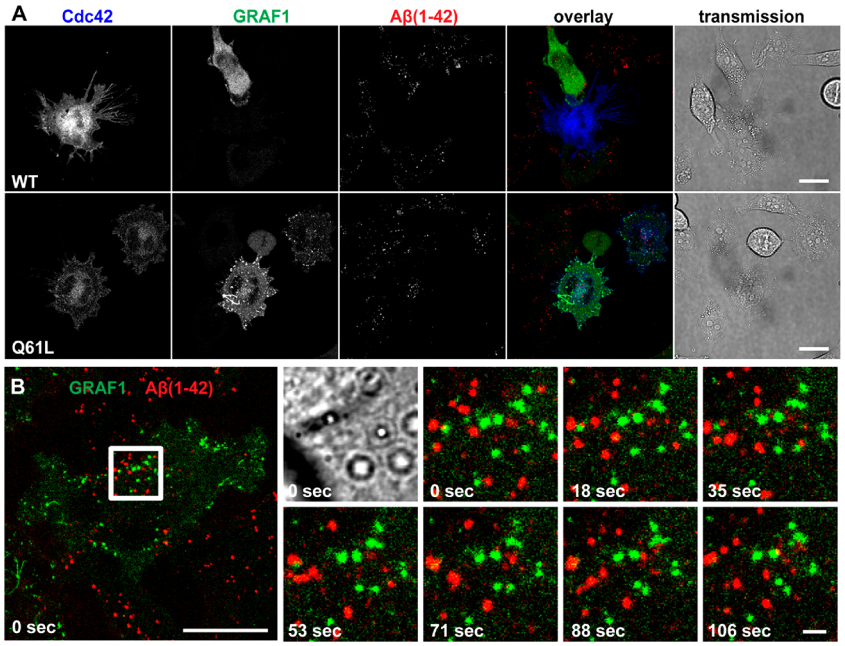

Figure 4. Uptake of Aβ(1-42) is independent of GRAF1 in HeLa cells. (A) HeLa Flp-In T-REx cells were induced to express GFP-tagged GRAF1 after transfection with either WT Cdc42 or DA Cdc42 Q61, both mCherry-tagged. The cells were incubated with 1 μM HF647-labeled Aβ(1-42) for 40 min, washed, and imaged by confocal microscopy. GRAF1 forms both punctate and tubular structures in cells expressing Cdc42 Q61L. Aβ(1-42) is not found to colocalize with these. The scale bars represent 20 μm. (B) Cells transfected with Cdc42 Q61L as in part A but exposed to a 15 min pulse of 5 μM Aβ(1-42) followed by time-lapse imaging by confocal microscopy. The whole-cell image (large image) shows the zoomed area (Cdc42 expression pattern depicted in Supplementary Figure S5), and small images are from the time lapse in Supplementary Movie 6. The scale bar is 20 μm in the whole-cell image and 2 μm in the zoomed-in images.

(5 μM) (Supplementary Figure S5), but we still did not observe colocalization. We also imaged GFP-GRAF1 and mCherry-Cdc42-Q61L positive cells by time-lapse microscopy with simultaneous detection of GRAF1 and Aβ(1-42) using a filter cube to split the signals (see snap-shots in Figure 4B and Supporting Movie 6). No apparent comovement of GRAF1- and Aβ(1-42)-containing vesicles was observed. Furthermore, GRAF1-positive vesicles appeared to be quite immobile compared to the Aβ(1-42)-containing endosomes, which moved rapidly. The conclusion is therefore that GRAF1 is not a mediator of Aβ(1-42) uptake. However, since the understanding of CLICs is not complete, it is still possible that Aβ(1-42) internalizes via this route, albeit under the regulation of alternative yet unidentified membrane sculpting proteins.

Involvement of Rho GTPases Cdc42, Rac1, and RhoA in Endocytosis of Aβ(1-42). Rho GTPases are important regulators of CIE (Figure 1).[30,41] When studying the role of GRAF1 in Aβ(1-42) uptake, we observed differences in the intensity and number of Aβ(1-42)-positive fluorescent foci in HeLa cells overexpressing WT and dominant active (Q61L) Cdc42 (Figure 4A), suggesting that this small Rho GTPase modulates uptake. Since Cdc42 (and other Rho GTPases) regulate the actin cytoskeleton,[74] this would be consistent with our previously published result that inhibitors of actin polymerization reduced Aβ(1-40) and Aβ(1-42) but not Trf internalization in SH-SY5Y cells.[13] To follow up on this finding, we explored systematically how Aβ(1-42) uptake depends on overexpression of WT, DN, and DA forms of Cdc42 as well as Rac1 and RhoA, which are two additional well-described Rho GTPases that furthermore have been implicated in AD pathology[31] and to some extent appear to be regulated by the presence of Aβ peptides.[57,58]

First, cells were transfected with EGFP-Cdc42 variants (WT, DN, DA), followed by 1 h treatment with 1 μM Aβ(1-42) (Figure 5A) or 5 min with 5 μg/mL Trf (Supplementary Figure S6). The EGFP-Cdc42 expressing cells have altered morphologies, with increased filopodia formation, consistent with the effect of Cdc42 on the actin skeleton.[74] Furthermore, the cell-to-cell variation in EGFP intensity shows that transfected cells expressed different amounts of the EGFP-Cdc42 variants, as confirmed by flow cytometry (Figure 5B). We took advantage of this when quantifying Aβ(1-42) and Trf uptake, by gating cells as nontransfected (overlapping with the intensity of mock cells transfected with MQ water, see Supplementary Figure S7) and low, medium, and high transfected (Figure 5B) based on their EGFP intensity, as previously described.[13] Within each gate, we determined the mean cellular fluorescence intensity of HF647-labeled Aβ(1-42) or AF647-labeled Trf (Figure 5C), allowing observation of concentration-dependent effects. We found that both Aβ(1-42) and Trf uptake is reduced by overexpression of DA EGFP-Cdc42 Q61L, suggesting that Cdc42 modulation can effect both CIE and CME. Control experiments showed that the uptake of dextran was unaffected (Supplementary Figure S8), confirming no effect on the intrinsic endocytic capacity of the cells. Overexpression of WT or DN EGFP-Cdc42 had no effect on Aβ(1-42) and Trf uptake (Figure 5C).

We repeated this set of experiments, exploring also the Rho GTPases Rac1 and RhoA. Overexpression of EGFP-tagged Rac1 (DA Q61L, WT, and DN T17N) induced lamellipodia-like morphologies in transfected cells as expected from the literature.[74] None of the Rac1 variants had any effect on Aβ(1-42) uptake (Figure 6A,B), not even at the highest levels of overexpression (see Supplementary Figure S10 for depiction of the flow cytometry gates), although a reduction of Trf uptake

https://dx.doi.org/10.1021/acschemneuro.0c00053
ACS Chem. Neurosci. 2020, 11, 1925−1936

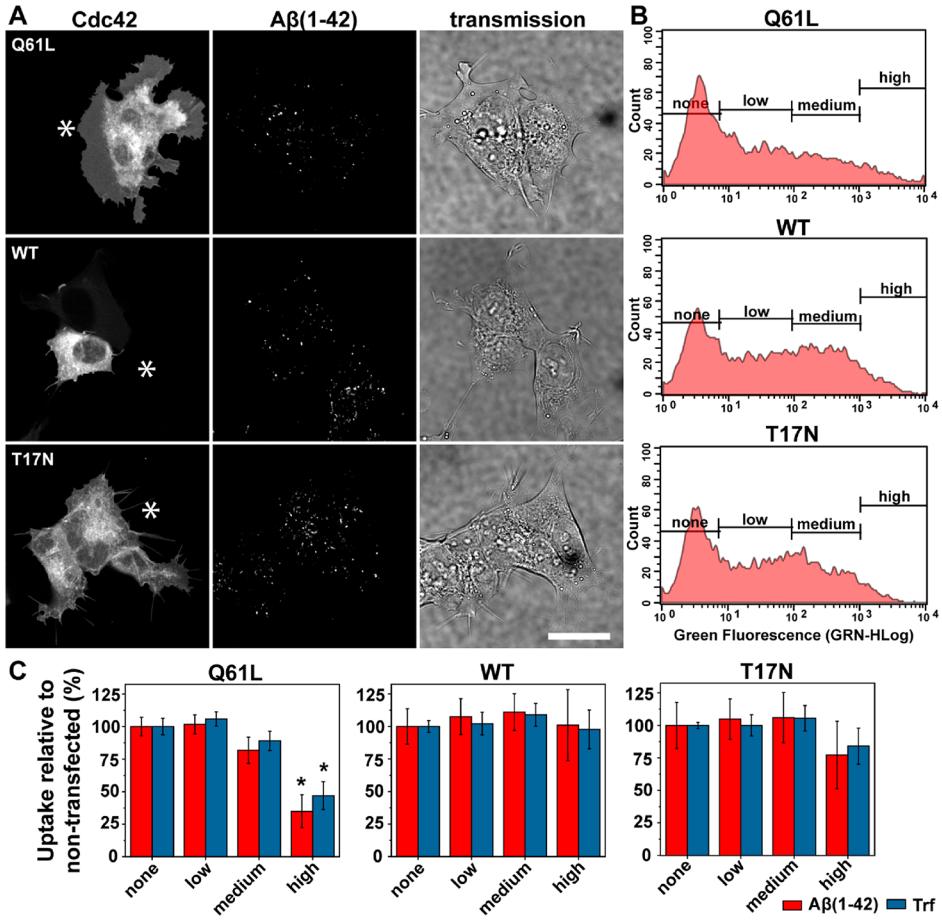

Figure 5. Cellular uptake of Aβ(1-42) is reduced by Cdc42 Q61L overexpression. (A) Confocal microscopy images of SH-SY5Y cells transfected with EGFP-tagged Cdc42 (DA Q61L, WT, or DN T17N) following incubation with 1 μM HF647-labeled Aβ(1-42) for 1 h. The scale bar is 20 μm and representative for all images. The asterisks (*) marks the positions of cells that are not expressing Cdc42. (B) Representative flow cytometry histograms (cell count vs intensity) of cells analyzed 24 h post transfection with EGFP-labeled Cdc42. For further analysis, the cells were gated for peptide uptake based on transfection efficiency and the extent of EGFP-Cdc42 overexpression (e.g., green fluorescence; none, low, medium, and high) as indicated in the figures. (C) Quantification of Aβ(1-42) and Trf uptake in cells transfected with Cdc42. The cells were incubated with either 1 μM HF647-labeled Aβ(1-42) for 1 h or 5 μg/mL AF647-labeled Trf for 5 min, washed, and analyzed for intracellular peptide signal by flow cytometry. Uptake is reported as relative mean cellular fluorescence in relation to uptake in nontransfected cells (N = 3, n = 4). Asterisk (*) marks uptake levels that are significantly different from uptake in nontransfected cells (adjusted p-value <0.05) by one-way ANOVA with matched data followed by multiple comparisons with Bonferroni posthoc test (adjusted p-values were Q61L, Aβ(1-42) none vs high 0.0001 and Trf none vs high <0.0001).

in the cells with the highest concentration of WT and DN Rac1 was observed. The latter result is contrasting observations by Lamaze et al.,[75] investigating Trf uptake in HeLa cells, highlighting how highly variable endocytic responses can be among cell types. We also observe that cells with a "medium" expression level of DA Rac1 appear to internalize slightly more Trf than control, suggesting that endocytic pathways may be sensitively fine-tuned by the transient concentration of adaptors. Modulation of Rac1 did not alter the endocytic capacity of cells, as measured by the uptake of dextran (Supplementary Figure S8). Considering the involvement of Cdc42 and Rac1 in macropinocytosis,[30] which we have previously inhibited by IPA-3 and wortmannin showing reductions in the uptake of Aβ(1-40) and Aβ(1-42),[13] it is noteworthy that we do not observe any effects on Aβ(1-42) uptake with Rac1. This is furthermore interesting in relation to a study showing that the uptake of fibrillar Aβ(1-42) by microglia depends on Rac1.[76] This points to differences in the uptake mechanisms of soluble and fibrillar Aβ forms. We have recently observed similar, seemingly mechanistic differences in the uptake of preformed fibril fragments and monomers of the Parkinson's disease related protein α-synuclein.[40]

Lastly, cells were transfected with EGFP-tagged RhoA (DA Q63L, WT, and DN T19N) and exposed to Aβ(1-42) and Trf, followed by analysis by confocal microscopy (Aβ(1-42) in Figure 7A, Trf in Supplementary Figure S11) and flow cytometry (Figure 7B, gates in Supplementary Figure S12). This showed that the uptake of both Aβ(1-42) and Trf is reduced following overexpression of all variants of RhoA. The most extensive concentration-dependent effect is seen with DA Q63L, but statistically significant reductions in uptake were also observed following overexpression of WT and T19N (T19N; high transfection gate not included due to too few cells). The uptake reduction in cells expressing DA RhoA could, at least partially, be explained by an overall decrease in endocytic activity as the uptake of dextran 10 kDa is reduced by up to 50% (Supplementary Figure S8). However, reports by Yu et al.[59] demonstrate involvement of RhoA in endocytosis of Aβ(1-42) oligomers, in-line with our results. Also, the results do not point toward any importance of fast endophilin-

https://dx.doi.org/10.1021/acschemneuro.0c00053
ACS Chem. Neurosci. 2020, 11, 1925−1936

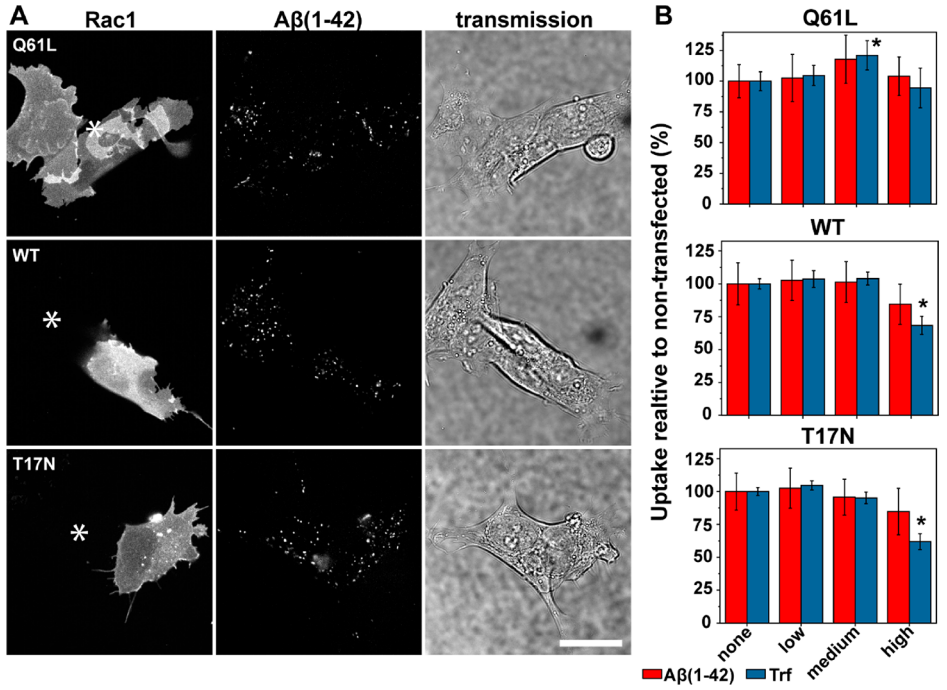

Figure 6. Cellular uptake of Aβ(1-42) is not sensitive to changes in Rac1 expression. (A) SH-SY5Y cells transfected with EGFP-tagged Rac1 (DA Q61L, WT, or DN T17N) and incubated with 1 μM HF647-labeled Aβ(1-42) for 1 h imaged by confocal microscopy. The scale bar is 20 μm. The asterisks (*) marks an example of a cell that is not expressing Rac1. (B) Quantification of Aβ(1-42) and Trf uptake in cells transfected with Rac1. The cells were incubated with either 1 μM HF647-labeled Aβ(1-42) or 5 μg/mL AF488-labeled Trf for 1 h or 5 min, respectively, washed and analyzed for intracellular peptide signal by flow cytometry. Uptake is reported as relative mean cellular fluorescence and based on level of Rac1-expression (none, low, medium, and high) in relation to uptake in nontransfected cells (N = 3, n = 4). The gates applied are displayed in Supplementary Figure S10. The asterisk (*) marks uptake levels that are significantly different from uptake in nontransfected cells (adjusted p-value <0.05) by one-way ANOVA with matched data followed by multiple comparisons with Bonferroni posthoc test (adjusted p-values were Q61L, Trf none vs medium 0.0355; WT, Trf none vs high 0.0001; T17N, Trf none vs high <0.0001).

mediated endocytosis (FEME)[45] in Aβ(1-42) internalization, as the uptake levels after perturbation of Rho GTPase activity are different compared to what would be expected if FEME (which is sensitive to perturbation of Rac1 and RhoA but activated upon Cdc42 inhibition[45]) was involved. This finding is also in-line with the dynamin-dependent nature of FEME and the demonstrated lack of involvement of dynamin in monomeric Aβ endocytosis.

CONCLUSION

In this study, we have used live cell confocal fluorescence microscopy and flow cytometry to study how perturbation of endocytic mechanisms that are sensitive to changes in membrane tension and the regulatory control of Rho GTPases influence the cellular uptake of monomeric Aβ(1-42). This extends previous work by us and others in this area and provides additional insight into cell biological mechanisms and pathways that contribute to the Alzheimer's disease relevant endolysosomal accumulations of Aβ(1-42).

We report that Aβ(1-42) uptake into SH-SY5Y cells is sensitive to osmotic pressure-induced alterations in membrane tension, which points to the involvement of CLICs or macropinocytosis. Importantly, Aβ(1-42) behaves distinctively different than the CME-cargo Trf, but also dextran, which is an unspecific fluid-phase endocytosis marker. This suggests that Aβ(1-42) uptake occurs by a specific and differently regulated uptake path. We have previously demonstrated that Aβ(1-42) uptake is sensitive to perturbations of actin,[13] which appears highly consistent with the findings here on the important regulatory roles of key CIE regulatory Rho GTPases. In previous work, we also observed reductions in Aβ(1-42) uptake upon pharmacological macropinocytosis inhibition.[13] Our observations of sensitivity to Cdc42 activity reinforce the putative importance of this path, although the lack of sensitivity to Rac1, an activator of the formation of the large membrane protrusions that drive the formation of macropinosomes,[30] suggests that macropinocytotic Aβ(1-42) uptake may be of a nonclassical type. The sensitivity to reduction of membrane tension could support macropinocytosis[53] but is mainly consistent with uptake via constitutively active CLIC/GEEC.[52] Importantly, we have previously observed polarized internalization of Aβ(1-42) in CHO cells, resulting from lamellipodia,[20] which are CLIC-enriched areas.[35] Furthermore, CLICs are important regulators of the cell uptake of the brain-abundant and AD-relevant glycosphingolipid GM1, which could be a putative receptor due to its reported tight binding to Aβ peptides,[41,49] influencing also their aggregation[77] and toxicity.[78] Notably, we have observed that NIH-3T3 fibroblasts internalize more Aβ(1-42) than CHO and SH-SY5Y, consistent with their inherent endocytic capacities.[13] We here note that fibroblasts, in particular, have an exceptionally high constitutive activation of CLICs.[35] Interestingly, in this regard, we find that Aβ(1-42) uptake is independent of the BAR domain containing and membrane sculpting protein GRAF1, which has been put forward as a key regulator of CLIC formation.[50,51]

Altogether, we report that Aβ(1-42) internalizes into cells via a specific and distinctive CIE mechanism that is highly sensitive to changes in membrane tension and the regulatory

https://dx.doi.org/10.1021/acschemneuro.0c00053
ACS Chem. Neurosci. 2020, 11, 1925−1936

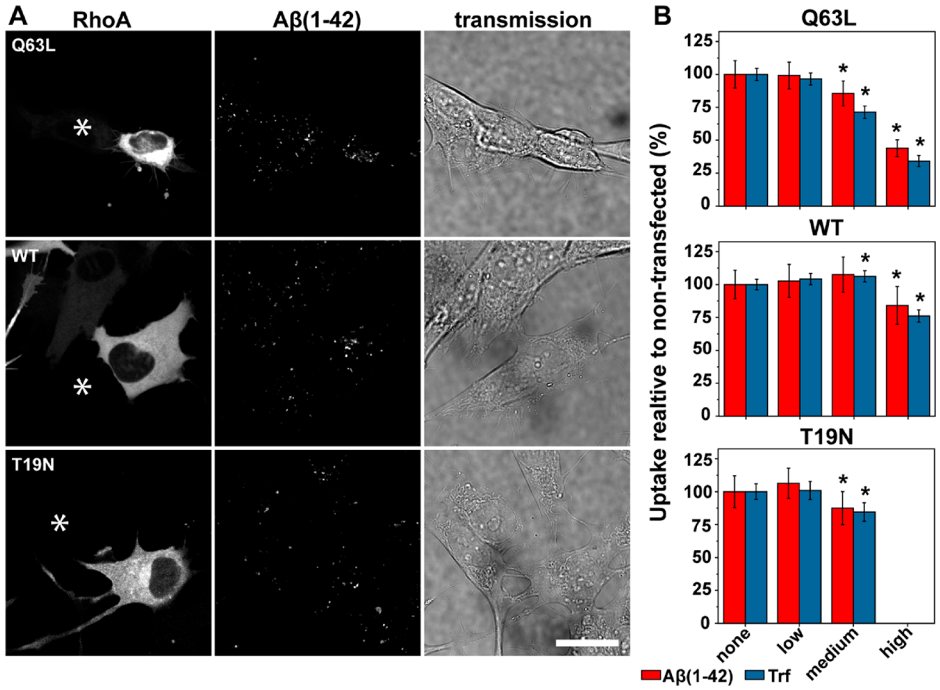

Figure 7. Cellular uptake of Aβ(1-42) is reduced by RhoA overexpression. (A) SH-SY5Y cells transfected with EGFP-tagged RhoA (DA Q63L, WT, or DN T19N) and incubated with 1 μM HF647-labeled Aβ(1-42) for 1 h imaged by confocal microscopy. The scale bar is 20 μm. The asterisks (*) mark an example of a cell that is not expressing RhoA. (B) Quantification of Aβ(1-42) and Trf uptake in cells transfected with RhoA. The cells were incubated with either 1 μM HF647-labeled Aβ(1-42) or 5 μg/mL AF647-labeled Trf for 1 h or 5 min, respectively, washed and analyzed for intracellular peptide signal by flow cytometry. Uptake is reported as relative mean cellular fluorescence and based on the level of RhoA-expression (none, low, medium, and high) in relation to uptake in nontransfected cells (N = 4, n = 4). T19N-transfected cells displayed few cells in the high transfected-gate, and this data was thus not included. The gates applied are displayed in Supplementary Figure S12. Asterisk (*) marks uptake levels that are significantly different from uptake in nontransfected cells (adjusted p-value <0.05) by one-way ANOVA with matched data followed by multiple comparisons with Bonferroni posthoc test (adjusted p-values were Q63L, Aβ(1-42) none vs medium 0.0013, none vs high <0.0001, Trf none vs medium <0.0001, none vs high <0.0001; WT, Aβ(1-42) none vs high 0.0224, Trf none vs medium 0.0059, none vs high <0.0001; T19N, Aβ(1-42) none vs medium 0.0098, Trf none vs medium 0.0003).

control of small Rho GTPases. The uptake mechanism appears similar to uptake via CLICs or possibly macropinocytosis, but the independence of Rac1 and GRAF1 suggests that it also involves yet uncharacterized membrane-sculpting and vesicle coating proteins of these incompletely characterized clathrin-independent endocytic paths. Better insights into this molecular machinery, guided by the results presented here, will undoubtedly provide a clearer cellular and molecular understanding of how uptake relates to endolysosomal intraneuronal Aβ accumulation. Putatively, this could also have important implications toward the development of future Aβ-clearing therapies, possibly targeting the endocytic path.

METHODS

Reagents. Synthetic Aβ(1-42) peptide, conjugated to the HiLyte Fluor HF488 or HF647 at the N-terminus, were from Anaspec Inc. (Fremont). The peptide purity was >95% as determined by Anaspec Inc. by MS and RP-HPLC. AlexaFluor488 (AF488)- and AlexaFluor647 (AF647)-labeled Transferrin (Trf) and AF647-labeled dextran 10 kDa were from Molecular Probes and purchased via ThermoFisher Scientific (Gothenburg, Sweden). The human neuroblastoma cell line SH-SY5Y was purchased from Sigma-Aldrich, and the Flp-In T-Rex HeLa cells were from Francis et al.[66] Cell culture reagents (minimal essential medium, nutrient mixture F-12 Ham, MEM nonessential amino acids, Dulbecco's Modified Eagles Medium, heat-inactivated fetal bovine serum, L-glutamine, and trypsin-EDTA 0.25%) and buffers (HEPES and DPBS) were from Gibco or Sigma-Aldrich, B-27 was from Gibco, and Lipofectamine 2000 was from Invitrogen and purchased via ThermoFisher Scientific. Doxycycline hyclate was from Sigma-Aldrich, and hygromycin B from Invitrogen and blasticidin S HCl from Gibco were both purchased via ThermoFisher Scientific. Plasmids encoding for EGFP-tagged Rho GTPases were from Addgene (Cdc42, Q61L no. 12986, WT no. 12975, T17N no. 12976; Rac1, Q61L no. 12981, WT no. 12980, T17N no. 12982; RhoA, Q63L no. 12968, WT no. 12965, T19N no. 12967), and mCherry-tagged Cdc42 WT and Q61L were from Francis et al.[66]

Preparation and Handling of Aβ(1-42). The lyophilized Aβ(1-42) peptide powders were dissolved in hexafluoro-2-propanol to disrupt any aggregates[79] and monomerize the peptide. The solutions were vortexed briefly and aliquoted at 4 °C. The solvent in each aliquot was evaporated at 37 °C for 15 min on a heating block and additional 45 min using a RVC 2-18 CD rotational vacuum concentrator (Martin Christ, Germany). The remaining peptide films were snap frozen in liquid nitrogen and kept at −80 °C until further use. We have demonstrated that this protocol results in highly monomeric samples.[13] For concentration determinations, the peptide film was dissolved in 1% ammonium hydroxide (v/v), and the absorption of the dye label was measured on a Cary 4000 UV−vis spectrophotometer (Agilent Technologies, Santa Clara, CA). Extinction coefficients of 70 000 M^{-1} cm^{-1} at 504 nm and 250 000 M^{-1} cm^{-1} at 649 nm was used for the HF488 and HF647 dye labels, respectively, according to the information provided by the manufacturer. Prior to each experiment, one peptide film was dissolved in a small volume 1% ammonium hydroxide (v/v) and diluted with cell culture medium supplemented with 2% B-27 and 30 mM HEPES. The concentration of ammonium hydroxide was kept below 0.01% and was matched in controls to ensure identical treatment of all samples. Unused samples were discarded in order to avoid Aβ(1-42) aggregation induced by freeze−thawing.

https://dx.doi.org/10.1021/acschemneuro.0c00053
ACS Chem. Neurosci. 2020, 11, 1925−1936

Cell Culture and Sample Preparation. *Cell Maintenance and Seeding.* SH-SY5Y cells were grown in a 1:1 mixture of minimal essential medium (MEM) and nutrient mixture F-12 Ham supplemented with 10% heat-inactivated fetal bovine serum, 1% MEM nonessential amino acids, and 2 mM L-glutamine. The cells were detached (trypsin-EDTA 0.25%, 5 min) and passaged twice a week. Cells were plated 1 day prior to experiments in either flat-bottomed 96 well plates (Nunc or VWR; 50 000 cells/well) for flow cytometry or in glass-bottomed culture dishes (MatTek; 25 000 cells (untreated cells) or 100 000 (transfected cells)/14 mm dish) for microscopy. Flp-In T-Rex HeLa cells with inducible expression of GFP-GRAF1[66] were grown in DMEM supplemented with 10% heat-inactivated fetal bovine serum, 2% L-glutamine, and with the addition of 100 μg/mL hygromycin B and 5 μg/mL blasticidin S HCl. The cells were detached (trypsin-EDTA 0.25%, 3 min) and passaged twice a week. Transfected cells were plated 1 day prior to experiments in glass-bottomed culture dishes (MatTek; 50 000 cells/14 mm dish) for microscopy.

Alterations in Membrane Tension. SH-SY5Y cells were incubated with Aβ(1-42), Trf, and dextran 10 kDa while exposed to changes in membrane tension and analyzed by confocal microscopy and flow cytometry. For uptake at isotonic conditions, the cells were washed 1× with serum-free medium, incubated with either 2 μM HF488-labeled Aβ(1-42), 5 μg/mL AF488-labeled Trf, or 250 μg/mL AF647-labeled dextran 10 kDa in serum-free medium with the addition of 2% B-27 for 10 min, washed 1× with serum free medium for microscopy, or 3×/2 min on ice with either ice-cold serum-free medium (Aβ(1-42) and dextran) or acidic buffer (0.1 M glycine-HCl buffer pH 2.5 with 150 mM NaCl; Trf)[80] and harvested for analysis by flow cytometry. For uptake at hypotonic conditions, the cells were first pretreated for 10 min in isotonic medium where after they were incubated with the peptides and dextran for 10 min as outlined above but diluted in hypotonic medium (25−75% MQ water added to the isotonic medium). Lastly, cells analyzed for uptake at recovery conditions were first pretreated with isotonic medium for 10 min followed by treatment in hypotonic medium for 10 min, whereupon they were exposed to the peptides and dextran in isotonic medium for 10 min.

Transfection of Rho GTPases and Induction of GRAF1 Expression. SH-SY5Y cells were passaged 2 days prior to transfection, grown to ∼70% confluency, and transfected with plasmids encoding for Rho GTPases (EGFP-tagged DA, WT, and DN variants of Cdc42, Rac1, and RhoA; see the above section Reagents) by electroporation using a Neon Transfection System (Invitrogen, Carlsbad, CA), following the protocol provided by the manufacturer and applying a single pulse of 1 100 V with a pulse width of 50 ms. The cells were transfected using 1 μg of plasmid DNA/100 000 cells in a 10 μL Neon Tip or 10 μg of plasmid DNA/10^6 cells in a 100 μL Neon Tip and plated immediately after. Based on the initial experiments, the analysis was set to ∼24 h, ∼27 h, and ∼30 h post-transfection for Cdc42, Rac1, and RhoA, respectively, by evaluating the time it took until the cells expressed the proteins and adapted the expected morphologies. The Flp-In T-Rex HeLa cells with inducible expression of GFP-GRAF1 were seeded in 6 well plates (250 000 cells/well) 24 h prior to induction. GFP-GRAF1 expression was induced by addition of 1 ng/mL doxycycline hyclate, and 3 h postinduction the cells were transfected with mCherry-tagged Cdc42 WT or DA Q61L by Lipofectamine 2000 (0.5 μg of DNA and 1 μL of Lipofectamine/well) following the protocol provided by the manufacturer. At 5 h post-transfection, the cells were harvested and reseeded in glass-bottomed dishes followed by Aβ exposure and imaging 24 h post-reseeding.

Confocal Microscopy. Confocal images were acquired on a Nikon C2+ confocal microscope equipped with a C2-DUVB GaAsP Detector Unit and using an oil-immersion 60× 1.4 Nikon APO objective (Nikon Instruments, Amsterdam, The Netherlands). The sample was excited and detected with appropriate excitation laser lines and emission filters, sequentially for samples including fluorophores excited at 488 nm, 561 nm, and 640 nm, or simultaneously using a filter cube to split the channels when imaging only fluorophores excited at 488 and 640 nm.

Flow Cytometry. Flow cytometry was used for quantification of cellular uptake. Prior to analysis, the cells were washed 3×/2 min in ice-cold serum free medium (Aβ(1-42) and dextran 10 kDa) or acidic buffer (0.1 M glycine-HCl buffer pH 2.5 with 150 mM NaCl; Trf) and detached by trypsin-EDTA 0.25% for 7 min followed by addition of ice-cold FBS-supplemented cell culture medium to inhibit further proteolytic degradation of the cells. All samples were kept on ice until they were analyzed on a Guava EasyCyte 8HT (Millipore, Darmstadt, Germany) that automatically retrieves samples from a 96-well plate. In order to exclude effects due to difference in delay time, we used mixed order of analysis, loading only a few samples at a time with the remaining samples kept on ice. Only the central cell cluster on the forward/side scatter (FSC/SSC) dot plot was analyzed, and for each sample 5 000 cells from within the gate were counted. The EGFP, HF488, and AF488 fluorophores were excited by a 488 nm laser, and fluorescence was detected through a 525/30 nm filter. HF647 and AF647 was excited with a 635 nm laser and detected through a 661/19 nm filter. The mean cellular uptake or level of Rho GTPase expression was estimated as the average fluorescence intensity of all cells within the gate. The mean cellular uptake was baseline corrected by subtracting the signal recorded for untreated cells. Each cell treatment was performed in three or four technical replicates (n = 3−4) and repeated on at least two separate occasions ($N \geq 2$). All flow cytometry data was analyzed in InCyte software (Millipore, Darmstadt, Germany) and displayed using Origin software (OriginLab, Northampton, MA).

Statistics. Statistical analysis was performed by matched sample ANOVA using GraphPad Prism software (GraphPad, San Diego, CA) on data that had been normalized so that the uptake in nontransfected cells was 100% for the individual experiments. Matched sample ANOVA was followed by multiple comparisons with the Bonferroni posthoc test to test for differences in mean peptide uptake between nontransfected cells and uptake at the different transfection efficiencies. This means that the reported individual p-values have been adjusted for the number of comparisons that were relevant to the experiment.

■ ASSOCIATED CONTENT

Supporting Information

The Supporting Information is available free of charge at https://pubs.acs.org/doi/10.1021/acschemneuro.0c00053.

Supplementary Movie 1, cellular exposure to Aβ(1-42) and dextran 10 kDa during isotonic conditions (AVI)

Supplementary Movie 2, cellular exposure to Aβ(1-42) and dextran 10 kDa during hypotonic conditions (AVI)

Supplementary Movie 3, cellular exposure to Aβ(1-42) and dextran 10 kDa during recovery conditions (AVI)

Supplementary Movie 4, tubulation and fission of dextran 10 kDa-filled VLDs (AVI)

Supplementary Movie 5, cellLight Actin-GFP staining of cells exposed to changes in membrane tension (AVI)

Supplementary Movie 6, Aβ(1-42) and GRAF1 in cells expressing Cdc42 Q61L (AVI)

Associated confocal microscopy movie descriptions and supporting confocal microscopy and flow cytometry data (PDF)

■ AUTHOR INFORMATION

Corresponding Author

Elin K. Esbjörner − *Division of Chemical Biology, Department of Biology and Biological Engineering, Chalmers University of Technology, 412 96 Gothenburg, Sweden;* orcid.org/0000-0002-1253-6342; Phone: +46 (0)31 772 5120; Email: eline@chalmers.se

https://dx.doi.org/10.1021/acschemneuro.0c00053
ACS Chem. Neurosci. 2020, 11, 1925−1936

Authors

Emelie Wesén − *Division of Chemical Biology, Department of Biology and Biological Engineering, Chalmers University of Technology, 412 96 Gothenburg, Sweden*

Richard Lundmark − *Department of Integrative Medical Biology, Umeå University, Umeå 901 87, Sweden*

Complete contact information is available at: https://pubs.acs.org/10.1021/acschemneuro.0c00053

Author Contributions

E.W. performed all the experiments. R.L. contributed cell lines and research tools. All authors contributed to conceiving the idea, planning the study, analysis of data, discussion of results, and reviewing the final manuscript. E.W. and E.K.E wrote the paper.

Notes

The authors declare no competing financial interest.

■ ACKNOWLEDGMENTS

This work was supported by grants to E.K.E from the Wenner-Gren Foundations, the Swedish Research Council (Grant 2016-03902), the Swedish Research Council funded Linneaus Centre SUPRA, and the Lundberg Foundation.

■ REFERENCES

(1) Glenner, G. G., and Wong, C. W. (1984) Alzheimer's disease: initial report of the purification and characterization of a novel cerebrovascular amyloid protein. *Biochem. Biophys. Res. Commun. 120*, 885−890.

(2) Masters, C. L., Simms, G., Weinman, N. A., Multhaup, G., McDonald, B. L., and Beyreuther, K. (1985) Amyloid plaque core protein in Alzheimer disease and Down syndrome. *Proc. Natl. Acad. Sci. U. S. A. 82*, 4245−4249.

(3) Grundke-Iqbal, I., Iqbal, K., Tung, Y. C., Quinlan, M., Wisniewski, H. M., and Binder, L. I. (1986) Abnormal phosphorylation of the microtubule-associated protein tau (tau) in Alzheimer cytoskeletal pathology. *Proc. Natl. Acad. Sci. U. S. A. 83*, 4913−4917.

(4) Hardy, J., and Allsop, D. (1991) Amyloid deposition as the central event in the aetiology of Alzheimer's disease. *Trends Pharmacol. Sci. 12*, 383−388.

(5) Nilsberth, C., Westlind-Danielsson, A., Eckman, C. B., Condron, M. M., Axelman, K., Forsell, C., Stenh, C., Luthman, J., Teplow, D. B., Younkin, S. G., Naslund, J., and Lannfelt, L. (2001) The' 'Arctic' APP mutation (E693G) causes Alzheimer's disease by enhanced Abeta protofibril formation. *Nat. Neurosci. 4*, 887−893.

(6) Sherrington, R., Rogaev, E. I., Liang, Y., Rogaeva, E. A., Levesque, G., Ikeda, M., Chi, H., Lin, C., Li, G., Holman, K., Tsuda, T., Mar, L., Foncin, J.-F., Bruni, A. C., Montesi, M. P., Sorbi, S., Rainero, I., Pinessi, L., Nee, L., Chumakov, I., Pollen, D., Brookes, A., Sanseau, P., Polinsky, R. J., Wasco, W., Da Silva, H. A. R., Haines, J. L., Pericak-Vance, M. A., Tanzi, R. E., Roses, A. D., Fraser, P. E., Rommens, J. M., and St George-Hyslop, P. H. (1995) Cloning of a gene bearing missense mutations in early-onset familial Alzheimer's disease. *Nature 375*, 754−760.

(7) Rovelet-Lecrux, A., Hannequin, D., Raux, G., Meur, N. L., Laquerriere, A., Vital, A., Dumanchin, C., Feuillette, S., Brice, A., Vercelletto, M., Dubas, F., Frebourg, T., and Campion, D. (2006) APP locus duplication causes autosomal dominant early-onset Alzheimer disease with cerebral amyloid angiopathy. *Nat. Genet. 38*, 24−26.

(8) Glenner, G. G., and Wong, C. W. (1984) Alzheimer's disease and Down's syndrome: sharing of a unique cerebrovascular amyloid fibril protein. *Biochem. Biophys. Res. Commun. 122*, 1131−1135.

(9) Deane, R., Sagare, A., Hamm, K., Parisi, M., Lane, S., Finn, M. B., Holtzman, D. M., and Zlokovic, B. V. (2008) apoE isoform-specific disruption of amyloid beta peptide clearance from mouse brain. *J. Clin. Invest. 118*, 4002−4013.

(10) Thinakaran, G., and Koo, E. H. (2008) Amyloid precursor protein trafficking, processing, and function. *J. Biol. Chem. 283*, 29615−29619.

(11) LaFerla, F. M., Green, K. N., and Oddo, S. (2007) Intracellular amyloid-beta in Alzheimer's disease. *Nat. Rev. Neurosci. 8*, 499−509.

(12) Hu, X., Crick, S. L., Bu, G., Frieden, C., Pappu, R. V., and Lee, J. M. (2009) Amyloid seeds formed by cellular uptake, concentration, and aggregation of the amyloid-beta peptide. *Proc. Natl. Acad. Sci. U. S. A. 106*, 20324−20329.

(13) Wesén, E., Jeffries, G. D. M., Matson Dzebo, M., and Esbjörner, E. K. (2017) Endocytic uptake of monomeric amyloid-beta peptides is clathrin- and dynamin-independent and results in selective accumulation of Abeta(1-42) compared to Abeta(1−40). *Sci. Rep. 7*, 2021.

(14) Esbjörner, E. K., Chan, F., Rees, E., Erdelyi, M., Luheshi, L. M., Bertoncini, C. W., Kaminski, C. F., Dobson, C. M., and Kaminski Schierle, G. S. (2014) Direct observations of amyloid beta self-assembly in live cells provide insights into differences in the kinetics of Abeta(1−40) and Abeta(1-42) aggregation. *Chem. Biol. 21*, 732−742.

(15) Friedrich, R. P., Tepper, K., Ronicke, R., Soom, M., Westermann, M., Reymann, K., Kaether, C., and Fändrich, M. (2010) Mechanism of amyloid plaque formation suggests an intracellular basis of Abeta pathogenicity. *Proc. Natl. Acad. Sci. U. S. A. 107*, 1942−1947.

(16) Clifford, P. M., Zarrabi, S., Siu, G., Kinsler, K. J., Kosciuk, M. C., Venkataraman, V., D'Andrea, M. R., Dinsmore, S., and Nagele, R. G. (2007) Abeta peptides can enter the brain through a defective blood-brain barrier and bind selectively to neurons. *Brain Res. 1142*, 223−236.

(17) Oddo, S., Caccamo, A., Smith, I. F., Green, K. N., and LaFerla, F. M. (2006) A dynamic relationship between intracellular and extracellular pools of Abeta. *Am. J. Pathol. 168*, 184−194.

(18) Bhowmik, D., MacLaughlin, C. M., Chandrakesan, M., Ramesh, P., Venkatramani, R., Walker, G. C., and Maiti, S. (2014) pH changes the aggregation propensity of amyloid-beta without altering the monomer conformation. *Phys. Chem. Chem. Phys. 16*, 885−889.

(19) Lindberg, D. J., Wesén, E., Björkeroth, J., Rocha, S., and Esbjörner, E. K. (2017) Lipid membranes catalyse the fibril formation of the amyloid-beta (1-42) peptide through lipid-fibril interactions that reinforce secondary pathways. *Biochim. Biophys. Acta, Biomembr. 1859*, 1921−1929.

(20) Wesén, E., Gallud, A., Paul, A., Lindberg, D. J., Malmberg, P., and Esbjörner, E. K. (2018) Cell surface proteoglycan-mediated uptake and accumulation of the Alzheimer's disease peptide Abeta(1-42). *Biochim. Biophys. Acta, Biomembr. 1860*, 2204−2214.

(21) Willen, K., Edgar, J. R., Hasegawa, T., Tanaka, N., Futter, C. E., and Gouras, G. K. (2017) Abeta accumulation causes MVB enlargement and is modelled by dominant negative VPS4A. *Mol. Neurodegener. 12*, 61.

(22) Näslund, J., Haroutunian, V., Mohs, R., Davis, K. L., Davies, P., Greengard, P., and Buxbaum, J. D. (2000) Correlation between elevated levels of amyloid beta-peptide in the brain and cognitive decline. *Jama 283*, 1571−1577.

(23) Knobloch, M., Konietzko, U., Krebs, D. C., and Nitsch, R. M. (2007) Intracellular Abeta and cognitive deficits precede beta-amyloid deposition in transgenic arcAbeta mice. *Neurobiol. Aging 28*, 1297−1306.

(24) Gouras, G. K., Tsai, J., Naslund, J., Vincent, B., Edgar, M., Checler, F., Greenfield, J. P., Haroutunian, V., Buxbaum, J. D., Xu, H., Greengard, P., and Relkin, N. R. (2000) Intraneuronal Abeta42 accumulation in human brain. *Am. J. Pathol. 156*, 15−20.

(25) Olsson, T. T., Klementieva, O., and Gouras, G. K. (2018) Prion-like seeding and nucleation of intracellular amyloid-beta. *Neurobiol. Dis. 113*, 1−10.

(26) Nath, S., Agholme, L., Kurudenkandy, F. R., Granseth, B., Marcusson, J., and Hallbeck, M. (2012) Spreading of neurodegenerative pathology via neuron-to-neuron transmission of beta-amyloid. *J. Neurosci. 32*, 8767−8777.

(27) Sandwall, E., O'Callaghan, P., Zhang, X., Lindahl, U., Lannfelt, L., and Li, J. P. (2010) Heparan sulfate mediates amyloid-beta internalization and cytotoxicity. *Glycobiology 20*, 533−541.
(28) Fu, Y., Zhao, J., Atagi, Y., Nielsen, H. M., Liu, C. C., Zheng, H., Shinohara, M., Kanekiyo, T., and Bu, G. (2016) Apolipoprotein E lipoprotein particles inhibit amyloid-beta uptake through cell surface heparan sulphate proteoglycan. *Mol. Neurodegener. 11*, 37.
(29) Kanekiyo, T., Zhang, J., Liu, Q., Liu, C. C., Zhang, L., and Bu, G. (2011) Heparan sulphate proteoglycan and the low-density lipoprotein receptor-related protein 1 constitute major pathways for neuronal amyloid-beta uptake. *J. Neurosci. 31*, 1644−1651.
(30) Qualmann, B., and Mellor, H. (2003) Regulation of endocytic traffic by Rho GTPases. *Biochem. J. 371*, 233−241.
(31) Bolognin, S., Lorenzetto, E., Diana, G., and Buffelli, M. (2014) The potential role of rho GTPases in Alzheimer's disease pathogenesis. *Mol. Neurobiol. 50*, 406−422.
(32) Doherty, G. J., and McMahon, H. T. (2009) Mechanisms of endocytosis. *Annu. Rev. Biochem. 78*, 857−902.
(33) Sandvig, K., Kavaliauskiene, S., and Skotland, T. (2018) Clathrin-independent endocytosis: an increasing degree of complexity. *Histochem. Cell Biol. 150*, 107−118.
(34) Bitsikas, V., Correa, I. R., Jr., and Nichols, B. J. (2014) Clathrin-independent pathways do not contribute significantly to endocytic flux. *eLife 3*, No. e03970.
(35) Howes, M. T., Kirkham, M., Riches, J., Cortese, K., Walser, P. J., Simpson, F., Hill, M. M., Jones, A., Lundmark, R., Lindsay, M. R., Hernandez-Deviez, D. J., Hadzic, G., McCluskey, A., Bashir, R., Liu, L., Pilch, P., McMahon, H., Robinson, P. J., Hancock, J. F., Mayor, S., and Parton, R. G. (2010) Clathrin-independent carriers form a high capacity endocytic sorting system at the leading edge of migrating cells. *J. Cell Biol. 190*, 675−691.
(36) Watanabe, S., Mamer, L. E., Raychaudhuri, S., Luvsanjav, D., Eisen, J., Trimbuch, T., Sohl-Kielczynski, B., Fenske, P., Milosevic, I., Rosenmund, C., and Jorgensen, E. M. (2018) Synaptojanin and Endophilin Mediate Neck Formation during Ultrafast Endocytosis. *Neuron 98*, 1184−1197.
(37) Sannerud, R., Declerck, I., Peric, A., Raemaekers, T., Menendez, G., Zhou, L., Veerle, B., Coen, K., Munck, S., De Strooper, B., Schiavo, G., and Annaert, W. (2011) ADP ribosylation factor 6 (ARF6) controls amyloid precursor protein (APP) processing by mediating the endosomal sorting of BACE1. *Proc. Natl. Acad. Sci. U. S. A. 108*, E559−568.
(38) Kang, Y. S., Zhao, X., Lovaas, J., Eisenberg, E., and Greene, L. E. (2009) Clathrin-independent internalization of normal cellular prion protein in neuroblastoma cells is associated with the Arf6 pathway. *J. Cell Sci. 122*, 4062−4069.
(39) Zeineddine, R., and Yerbury, J. J. (2015) The role of macropinocytosis in the propagation of protein aggregation associated with neurodegenerative diseases. *Front. Physiol. 6*, 277.
(40) Zhang, X., Wesén, E., Kumar, R., Bernson, D., Gallud, A., Paul, A., Wittung-Stafshede, P., and Esbjörner, E. K. (2020) Correlation between Cellular Uptake and Cytotoxicity of Fragmented alpha-Synuclein Amyloid Fibrils Suggests Intracellular Basis for Toxicity. *ACS Chem. Neurosci. 11*, 233−241.
(41) Ferreira, A. P. A., and Boucrot, E. (2018) Mechanisms of Carrier Formation during Clathrin-Independent Endocytosis. *Trends Cell Biol. 28*, 188−200.
(42) Kerr, M. C., and Teasdale, R. D. (2009) Defining macropinocytosis. *Traffic 10*, 364−371.
(43) Yoshida, S., Pacitto, R., Inoki, K., and Swanson, J. (2018) Macropinocytosis, mTORC1 and cellular growth control. *Cell. Mol. Life Sci. 75*, 1227−1239.
(44) Åmand, H. L., Fant, K., Nordén, B., and Esbjörner, E. K. (2008) Stimulated endocytosis in penetratin uptake: effect of arginine and lysine. *Biochem. Biophys. Res. Commun. 371*, 621−625.
(45) Boucrot, E., Ferreira, A. P., Almeida-Souza, L., Debard, S., Vallis, Y., Howard, G., Bertot, L., Sauvonnet, N., and McMahon, H. T. (2015) Endophilin marks and controls a clathrin-independent endocytic pathway. *Nature 517*, 460−465.
(46) Llobet, A., Gallop, J. L., Burden, J. J. E., Camdere, G., Chandra, P., Vallis, Y., Hopkins, C. R., Lagnado, L., and McMahon, H. T. (2011) Endophilin drives the fast mode of vesicle retrieval in a ribbon synapse. *J. Neurosci. 31*, 8512−8519.
(47) Sabharanjak, S., Sharma, P., Parton, R. G., and Mayor, S. (2002) GPI-anchored proteins are delivered to recycling endosomes via a distinct cdc42-regulated, clathrin-independent pinocytic pathway. *Dev. Cell 2*, 411−423.
(48) Kirkham, M., Fujita, A., Chadda, R., Nixon, S. J., Kurzchalia, T. V., Sharma, D. K., Pagano, R. E., Hancock, J. F., Mayor, S., and Parton, R. G. (2005) Ultrastructural identification of uncoated caveolin-independent early endocytic vehicles. *J. Cell Biol. 168*, 465−476.
(49) Fantini, J., Yahi, N., and Garmy, N. (2013) Cholesterol accelerates the binding of Alzheimer's beta-amyloid peptide to ganglioside GM1 through a universal hydrogen-bond-dependent sterol tuning of glycolipid conformation. *Front. Physiol. 4*, 120.
(50) Lundmark, R., Doherty, G. J., Howes, M. T., Cortese, K., Vallis, Y., Parton, R. G., and McMahon, H. T. (2008) The GTPase-activating protein GRAF1 regulates the CLIC/GEEC endocytic pathway. *Curr. Biol. 18*, 1802−1808.
(51) Holst, M. R., Vidal-Quadras, M., Larsson, E., Song, J., Hubert, M., Blomberg, J., Lundborg, M., Landström, M., and Lundmark, R. (2017) Clathrin-Independent Endocytosis Suppresses Cancer Cell Blebbing and Invasion. *Cell Rep. 20*, 1893−1905.
(52) Thottacherry, J. J., Kosmalska, A. J., Kumar, A., Vishen, A. S., Elosegui-Artola, A., Pradhan, S., Sharma, S., Singh, P. P., Guadamillas, M. C., Chaudhary, N., Vishwakarma, R., Trepat, X., Del Pozo, M. A., Parton, R. G., Rao, M., Pullarkat, P., Roca-Cusachs, P., and Mayor, S. (2018) Mechanochemical feedback control of dynamin independent endocytosis modulates membrane tension in adherent cells. *Nat. Commun. 9*, 4217.
(53) Loh, J., Chuang, M. C., Lin, S. S., Joseph, J., Su, Y. A., Hsieh, T. L., Chang, Y. C., Liu, A. P., and Liu, Y. W. (2019) An acute decrease in plasma membrane tension induces macropinocytosis via PLD2 activation. *J. Cell Sci. 132*, jcs232579.
(54) Vidal-Quadras, M., Holst, M. R., Francis, M. K., Larsson, E., Hachimi, M., Yau, W. L., Peränen, J., Martin-Belmonte, F., and Lundmark, R. (2017) Endocytic turnover of Rab8 controls cell polarization. *J. Cell Sci. 130*, 1147−1157.
(55) Stankiewicz, T. R., and Linseman, D. A. (2014) Rho family GTPases: key players in neuronal development, neuronal survival, and neurodegeneration. *Front. Cell. Neurosci. 8*, 314.
(56) Borin, M., Saraceno, C., Catania, M., Lorenzetto, E., Pontelli, V., Paterlini, A., Fostinelli, S., Avesani, A., Di Fede, G., Zanusso, G., Benussi, L., Binetti, G., Zorzan, S., Ghidoni, R., Buffelli, M., and Bolognin, S. (2018) Rac1 activation links tau hyperphosphorylation and Abeta dysmetabolism in Alzheimer's disease. *Acta Neuropathol. Commun. 6*, 61.
(57) Petratos, S., Li, Q. X., George, A. J., Hou, X., Kerr, M. L., Unabia, S. E., Hatzinisiriou, I., Maksel, D., Aguilar, M. I., and Small, D. H. (2008) The beta-amyloid protein of Alzheimer's disease increases neuronal CRMP-2 phosphorylation by a Rho-GTP mechanism. *Brain 131*, 90−108.
(58) Mendoza-Naranjo, A., Gonzalez-Billault, C., and Maccioni, R. B. (2007) Abeta1-42 stimulates actin polymerization in hippocampal neurons through Rac1 and Cdc42 Rho GTPases. *J. Cell Sci. 120*, 279−288.
(59) Yu, C., Nwabuisi-Heath, E., Laxton, K., and Ladu, M. J. (2010) Endocytic pathways mediating oligomeric Abeta42 neurotoxicity. *Mol. Neurodegener. 5*, 19.
(60) Aguilar, B. J., Zhu, Y., and Lu, Q. (2017) Rho GTPases as therapeutic targets in Alzheimer's disease. *Alzheimer's Res. Ther. 9*, 97.
(61) Gamba, P., Testa, G., Sottero, B., Gargiulo, S., Poli, G., and Leonarduzzi, G. (2012) The link between altered cholesterol metabolism and Alzheimer's disease. *Ann. N. Y. Acad. Sci. 1259*, 54−64.
(62) Askarova, S., Yang, X., and Lee, J. C. (2011) Impacts of membrane biophysics in Alzheimer's disease: from amyloid precursor

https://dx.doi.org/10.1021/acschemneuro.0c00053
ACS Chem. Neurosci. 2020, 11, 1925−1936

protein processing to abeta Peptide-induced membrane changes. *Int. J. Alzheimer's Dis. 2011*, 134971.
(63) Pietuch, A., Bruckner, B. R., and Janshoff, A. (2013) Membrane tension homeostasis of epithelial cells through surface area regulation in response to osmotic stress. *Biochim. Biophys. Acta, Mol. Cell Res. 1833*, 712−722.
(64) Dai, J., Sheetz, M. P., Wan, X., and Morris, C. E. (1998) Membrane tension in swelling and shrinking molluscan neurons. *J. Neurosci. 18*, 6681−6692.
(65) Colom, A., Derivery, E., Soleimanpour, S., Tomba, C., Molin, M. D., Sakai, N., González-Gaitán, M., Matile, S., and Roux, A. (2018) A fluorescent membrane tension probe. *Nat. Chem. 10*, 1118−1125.
(66) Francis, M. K., Holst, M. R., Vidal-Quadras, M., Henriksson, S., Santarella-Mellwig, R., Sandblad, L., and Lundmark, R. (2015) Endocytic membrane turnover at the leading edge is driven by a transient interaction between Cdc42 and GRAF1. *J. Cell Sci. 128*, 4183−4195.
(67) Li, L., Wan, T., Wan, M., Liu, B., Cheng, R., and Zhang, R. (2015) The effect of the size of fluorescent dextran on its endocytic pathway. *Cell Biol. Int. 39*, 531−539.
(68) Kosmalska, A. J., Casares, L., Elosegui-Artola, A., Thottacherry, J. J., Moreno-Vicente, R., Gonzalez-Tarrago, V., Del Pozo, M. A., Mayor, S., Arroyo, M., Navajas, D., Trepat, X., Gauthier, N. C., and Roca-Cusachs, P. (2015) Physical principles of membrane remodelling during cell mechanoadaptation. *Nat. Commun. 6*, 7292.
(69) Morris, C. E., and Homann, U. (2001) Cell surface area regulation and membrane tension. *J. Membr. Biol. 179*, 79−102.
(70) Reuzeau, C., Mills, L. R., Harris, J. A., and Morris, C. E. (1995) Discrete and reversible vacuole-like dilations induced by osmomechanical perturbation of neurons. *J. Membr. Biol. 145*, 33−47.
(71) Traub, L. M. (2009) Tickets to ride: selecting cargo for clathrin-regulated internalization. *Nat. Rev. Mol. Cell Biol. 10*, 583−596.
(72) Gorodinsky, A., and Harris, D. A. (1995) Glycolipid-anchored proteins in neuroblastoma cells form detergent-resistant complexes without caveolin. *J. Cell Biol. 129*, 619−627.
(73) Tamma, G., Procino, G., Svelto, M., and Valenti, G. (2007) Hypotonicity causes actin reorganization and recruitment of the actin-binding ERM protein moesin in membrane protrusions in collecting duct principal cells. *Am. J. Physiol. Cell Physiol. 292*, C1476−1484.
(74) Hall, A. (1998) Rho GTPases and the actin cytoskeleton. *Science 279*, 509−514.
(75) Lamaze, C., Chuang, T. H., Terlecky, L. J., Bokoch, G. M., and Schmid, S. L. (1996) Regulation of receptor-mediated endocytosis by Rho and Rac. *Nature 382*, 177−179.
(76) Kitamura, Y., Shibagaki, K., Takata, K., Tsuchiya, D., Taniguchi, T., Gebicke-Haerter, P. J., Miki, H., Takenawa, T., and Shimohama, S. (2003) Involvement of Wiskott-Aldrich syndrome protein family verprolin-homologous protein (WAVE) and Rac1 in the phagocytosis of amyloid-beta(1-42) in rat microglia. *J. Pharmacol. Sci. 92*, 115−123.
(77) Cebecauer, M., Hof, M., and Amaro, M. (2017) Impact of GM1 on Membrane-Mediated Aggregation/Oligomerization of beta-Amyloid: Unifying View. *Biophys. J. 113*, 1194−1199.
(78) Yanagisawa, M., Ariga, T., and Yu, R. K. (2010) Cytotoxic effects of G(M1) ganglioside and amyloid beta-peptide on mouse embryonic neural stem cells. *ASN Neuro 2*, No. e00029.
(79) Stine, W. B., Jr., Dahlgren, K. N., Krafft, G. A., and LaDu, M. J. (2003) In vitro characterization of conditions for amyloid-beta peptide oligomerization and fibrillogenesis. *J. Biol. Chem. 278*, 11612−11622.
(80) Kirchhausen, T., Macia, E., and Pelish, H. E. (2008) Use of dynasore, the small molecule inhibitor of dynamin, in the regulation of endocytosis. *Methods Enzymol. 438*, 77−93.

https://dx.doi.org/10.1021/acschemneuro.0c00053
ACS Chem. Neurosci. 2020, 11, 1925−1936